Ca^{2+} block and flickering both contribute to the negative slope of the IV curve in BK channels

Indra Schroeder,[1] Gerhard Thiel,[1] and Ulf-Peter Hansen[2]

[1]Plant Membrane Biophysics, Technical University of Darmstadt, 64287 Darmstadt, Germany
[2]Department of Structural Biology, University of Kiel, 24098 Kiel, Germany

Single-channel current–voltage (IV) curves of human large-conductance, voltage- and Ca^{2+}-activated K^+ (BK) channels are quite linear in 150 mM KCl. In the presence of Ca^{2+} and/or Mg^{2+}, they show a negative slope conductance at high positive potentials. This is generally explained by a Ca^{2+}/Mg^{2+} block as by Geng et al. (2013. *J. Gen. Physiol.* http://dx.doi.org/10.1085/jgp.201210955) in this issue. Here, we basically support this finding but add a refinement: the analysis of the open-channel noise by means of β distributions reveals what would be found if measurements were done with an amplifier of sufficient temporal resolution (10 MHz), namely that the block by 2.5 mM Ca^{2+} and 2.5 mM Mg^{2+} per se would only cause a saturating curve up to +160 mV. Further bending down requires the involvement of a second process related to flickering in the microsecond range. This flickering is hardly affected by the presence or absence of Ca^{2+}/Mg^{2+}. In contrast to the experiments reported here, previous experiments in BK channels (Schroeder and Hansen. 2007. *J. Gen. Physiol.* http://dx.doi.org/10.1085/jgp.200709802) showed saturating IV curves already in the absence of Ca^{2+}/Mg^{2+}. The reason for this discrepancy could not be identified so far. However, the flickering component was very similar in the old and new experiments, regardless of the occurrence of noncanonical IV curves.

The Journal of General Physiology

INTRODUCTION

In the presence of Ca^{2+} and Mg^{2+}, a negative slope conductance occurs in the IV curves of single large-conductance, voltage- and Ca^{2+}-activated K^+ (BK) channels. This has been shown in this issue in the Communication by Geng et al. and in previous studies (Ferguson, 1991; Morales et al., 1996; Zhang et al., 2006). Without divalent cations, the IV curves are quite linear; a minor sublinearity is partially assigned to a proton block (Brelidze and Magleby, 2004). These findings in BK channels support the general view that blocking by intracellular ions is the origin of negative slopes in the IV curves from K^+ channels in animal cells (Na^+: Yellen, 1984; Kehl, 1996; Morales et al., 1996; Ca^{2+} and/or Mg^{2+}: Ferguson 1991; Xia et al., 2004; Zhang et al., 2006; Geng et al., 2013) and in plant cells (Na^+: Weise and Gradmann, 2000; Cs^+: Draber and Hansen, 1994).

In contrast, we reported previously that human BK channels (α plus β1 subunit) stably expressed in HEK293 cells showed a negative slope conductance at high positive voltages even in the absence of divalent cations or other obvious potential blockers in a solution of 150 mM KCl and 10 mM EDTA (Schroeder and Hansen, 2007). However, the channels were still strongly activated by Ca^{2+} and Mg^{2+}, as it is characteristic for BK channels (Xia et al., 2002; Magleby, 2003; Orio and Latorre, 2005).

Because of this discrepancy, we repeated the experiments in another laboratory. Single-channel measurements were done on the same cell line in the absence and presence of Ca^{2+} and Mg^{2+}, as in the experiments of Schroeder and Hansen (2007). In the new experiments, we now found the traditional result: a nearly linear IV curve in the absence of Ca^{2+}/Mg^{2+}, and a negative slope in their presence.

Three questions arise from this finding. First, what has caused the unusual IV curves in the experiments of Schroeder and Hansen (2007)? Second, is the analysis of flickering based on the excess noise of the open state (Schroeder and Hansen, 2007) still valid? Third, does the analysis of flickering refine the picture of the Ca^{2+}/Mg^{2+} block?

With respect to the first question, we show some new measurements and report on some rare observations, which may indicate that not only contaminations in the solutions but also different culturing conditions have to be considered. However, because of the long temporal distance between the experiments (2006 and now), we are not able to give a definite answer.

The second question is by far of greater importance for us because the answer affects the validity of the analysis in Schroeder and Hansen (2007). The answer could easily be obtained if a noise-free patch-clamp amplifier

Correspondence to Indra Schroeder: schroeder@bio.tu-darmstadt.de

Abbreviation used in this paper: BK, large-conductance, voltage- and Ca^{2+}-activated K^+.

The Rockefeller University Press $30.00
J. Gen. Physiol. Vol. 141 No. 4 499–505
www.jgp.org/cgi/doi/10.1085/jgp.201210956

were available with sufficient bandwidth of, for example, 10 MHz. It would show the true value of the single-channel current (and not a reduced apparent level resulting from averaging over undetected fast flickering) and would deliver the rate constants of the normally undetected fast transitions between levels of different conductivity. Such an amplifier does not exist, but fortunately there is a mathematical approach, which can yield the same data (albeit with a little bit more scatter of the rate constants in the microsecond range). This tool is provided by the analysis of the excess of the open-channel noise by means of so-called β distributions (FitzHugh, 1983; Yellen, 1984; Heinemann and Sigworth, 1991; Weise and Gradmann, 2000; Schroeder and Hansen, 2006). The approach is powerful, as it can look far beyond the filter frequency of the amplifier. However, it is rarely used, maybe because of the highly interactive and time-consuming fitting process.

The analysis of the excess noise in the case of the BK channel yields the answer to the second question. The flickering process is the same in the previous experiments (Schroeder and Hansen, 2007) and in the new ones; it is not affected by the strange behavior of the IV curves in the absence of Ca^{2+}/Mg^{2+} in those previous experiments. The answer to the third question implies that the IV curve measured in the presence of 2.5 mM Ca^{2+} and 2.5 mM Mg^{2+} would show a weaker bending if measured with a 10-MHz amplifier than with the real 20-kHz amplifier.

MATERIALS AND METHODS

Electrophysiological measurements

Patch-clamp measurements were performed on inside-out patches of the same strain of HEK293 cells already used by Schroeder and Hansen (2007), stably expressing an hBK α-GFP construct and the β1 subunit (Lu et al., 2006). The cells were provided by U. Seydel and A. Schromm (Research Center Borstel, Borstel, Germany). The same solutions were used in the pipette and in the bath. The solution without divalent cations contained 150 mM KCl and 10 mM HEPES, with pH titrated with KOH to 7.2. In most experiments, no buffers for divalent ions were used because small (up to some micromolar) amounts of contaminating Ca^{2+}/Mg^{2+} do not cause a significant block (Cox et al., 1997). 2.5 mM $CaCl_2$ and 2.5 mM $MgCl_2$, 10 mM H-EDTA, 10 mM Na_2-EDTA, or 20 mM NaCl were added as indicated in the text. Patch electrodes were made from borosilicate glass (Science Products) coated internally with Sigmacote (Sigma-Aldrich), drawn on a PP-830 puller (Narishige), and dried overnight at 55°C. Single-channel currents under steady-state conditions were recorded by an amplifier (3900A; Dagan) with a four-pole anti-aliasing filter (Bessel) of 20 kHz. Data were stored on disc with a sampling rate of 100 kHz and analyzed with custom-made programs and Origin software (OriginLab Corporation). Liquid junction potential was not corrected because it was <5 mV in all experiments.

IV relationships (IV curves) were obtained from time series of 1- or 10-s duration, with the holding potential being increased from −200 mV in steps of 20 mV until +200 mV (or less, when the seal broke). Before the analysis of the fast flickering, artifacts (e.g., resulting from baseline drift, membrane instability, or amplifier discharge) were manually removed from the time series in the laboratory-made program *KielPatch* to avoid deformations of the β distributions. Minor peaks related to a second fast flickering process in the 10-µs range could not be eliminated and caused a second slope at the bottom of the amplitude histogram. However, Schroeder and Hansen (2009b) have shown that they are ignored by the fitting routine without affecting the values of the rate constants in the microsecond range of the fast gating process.

Evaluation of fast flickering: β fit

As described in our previous papers (Schroeder and Hansen, 2006, 2007, 2008, 2009b), a truncated two-state Markov model (Eq. 1) was sufficient for describing the fast flickering processes investigated here:

$$C \underset{k_{OC}}{\overset{k_{CO}}{\rightleftharpoons}} O. \quad (1)$$

In brief, the open-point histogram (distribution-per-level, Schröder et al., 2004) of the apparent open state (excluding visible closed states) was obtained from the measured time series by means of a Hinkley detector included in the program *KielPatch* (Schultze and Draber, 1993). For fitting the theoretical open-point histogram to the measured one, the laboratory-made program *bownhill* was used (β fit, FitzHugh, 1983; Yellen, 1984; Heinemann and Sigworth, 1991). Because the theory of β distributions did not provide any simple analytical approach (Riessner, 1998) for filters of higher order (e.g., four-pole Bessel filters), the theoretical amplitude histogram was generated from time series simulated on the basis of the model in Eq. 1. The true single-channel current I_{true} was suggested by an interactive dialog, and the rate constants k_{CO} and k_{OC} were determined by the fitting algorithm. The error sum for the best fit of k_{OC} and k_{CO} for a suggested I_{true} plotted versus I_{true} showed a minimum for the best value of I_{true} (Schroeder and Hansen, 2007; Abenavoli et al., 2009; Brauser et al., 2012). From this best fit, the parameters of the model in Eq. 1 were taken.

RESULTS AND DISCUSSION

Negative slopes in the IV curves are not observed in the absence of Ca^{2+} and Mg^{2+} in the new experiments

As mentioned in the Introduction, we previously reported that the IV curves from BK channels were identical with and without intracellular Ca^{2+}/Mg^{2+} (Schroeder and Hansen, 2007), showing negative slopes at positive potentials and greatly reduced single-channel conductance of 170 pS in the range of −80 to +80 mV (Fig. 1 B, blue symbols, labeled "Ki"). This is in contrast to the finding of quite linear IV curves in the absence of divalent cations by other workers (Ferguson, 1991; Morales et al., 1996; Zhang et al., 2006; Geng et al., 2013), and also to the values of conductance reported for BK channels in the absence of blockers, i.e., ∼250–300 pS (Ferguson, 1991; Cox et al., 1997; Magleby, 2003). In spite of this discrepancy, Schroeder and Hansen (2007) found a very strong shift in half-activation potential (−100 ± 3 mV with and +174 ± 14 mV without Ca^{2+}/Mg^{2+}, similar to the values of Orio and Latorre, 2005, and Xia et al., 2002). Because of the contrast regarding the IV curves, we repeated the experiments in a different laboratory (Darmstadt instead of Kiel).

The new experiments did not show a negative slope in the absence of Ca^{2+}/Mg^{2+} (Fig. 1 B, open black squares), and the slope conductance was 280 pS. The half-activation potential ($V_{1/2}$) in 150 mM KCl without added divalent ions or chelators was +57 ± 3 mV. The addition of 2.5 mM Ca^{2+} and Mg^{2+} each shifted $V_{1/2}$ to −76 ± 13 mV (not depicted). This shift indicated very low contamination by Ca^{2+}/Mg^{2+}, even without EDTA. BK channels are strongly Ca^{2+} activated in the micromolar range (Pallotta et al., 1981; Cox et al., 1997; Rothberg and Magleby, 2000; Xia et al., 2002; Magleby, 2003; Orio and Latorre, 2005; Piskorowski and Aldrich, 2006). In the case of Mg^{2+}, however, millimolar concentrations are required (Xia et al., 2002; Magleby, 2003; Yang et al., 2006; Zhang et al., 2006).

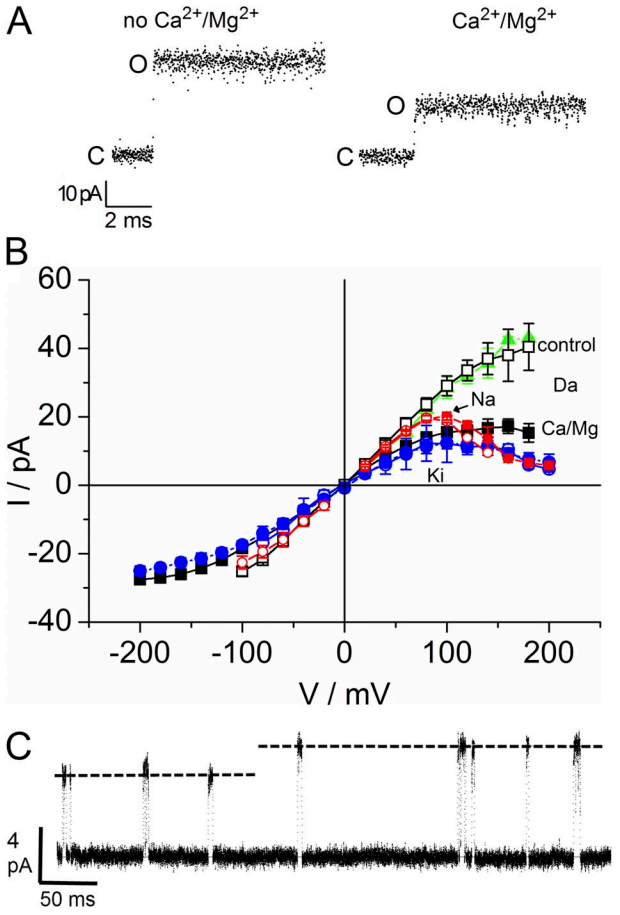

Figure 1. Influence of 2.5 mM Ca^{2+} and 2.5 mM Mg^{2+} on human BK channels. (A) New single-channel recordings measured at +140 mV with a 20-kHz filter illustrating the effect of 2.5 mM Ca^{2+} and Mg^{2+} on apparent single-channel current and noise. "O" and "C" mark the open and closed channel, respectively. (B) IV curves without (open black squares) and with (closed black squares) 2.5 mM Ca^{2+}/Mg^{2+} obtained from the recent experiments, labeled "Da." The IV curve in the presence of 10 mM H-EDTA is shown in green. As a comparison, the IV curves reported by Schroeder and Hansen (2007) are shown ("Ki," blue). Those ones measured with (closed circles) and without Ca^{2+}/Mg^{2+} (open circles) coincide. The red curves were obtained in Ca^{2+}/Mg^{2+}-free medium with 20 mM $NaCl_2$ (open circles) or Na_2-EDTA (closed squares). (C) A rare observation of spontaneous switching from the "Ki-type" (old) to the "Da-type" (recent). Data were acquired with a 20-kHz filter at +40 mV in 150 mM KCl plus 10 mM H-EDTA. A five-point moving average was used to generate the figure. Dashed lines mark the two different open states.

Adding 2.5 mM each of Ca^{2+} and Mg^{2+} led to a negative slope at high positive voltages and a reduction of single-channel conductance from 280 to 190 pS in the range of −80 to +80 mV (Fig. 1 B, closed black squares, labeled "Da"). Our recent experiments are thus consistent with those of Geng et al. (2013), who have found in the absence of Ca^{2+}/Mg^{2+} a large conductance of ∼250 pS at +100 mV with no negative slope, and in the presence of Ca^{2+}/Mg^{2+} a reduced conductance of 135 pS and a negative slope. (The negative slope reported by Geng et al., 2013 appears somewhat more pronounced than in Fig. 1 B, because Geng et al. have recorded currents at higher potentials.) Thus, our recent investigations yield the canonical experimental result, consistent with the findings of Geng et al. (2013) and others (Ferguson, 1991; Morales et al., 1996; Zhang et al., 2006).

Search for the origin of the discrepancy between the old ("Ki") and recent experiments ("Da")

A puzzling feature of the previous experiments was that Ca^{2+}/Mg^{2+} did not show any influence on the IV curves but a very pronounced effect on the activation curve (Fig. 7 in Schroeder and Hansen, 2007), which was similar to the shifts reported by other authors (Xia et al., 2002; Magleby, 2003; Orio and Latorre, 2005). Thus, the unknown condition causing the noncanonical behavior (Fig. 1 B, "Ki") mimicked the effect of Ca^{2+}/Mg^{2+} on the IV curve, but not on the voltage-dependent gating, indicating that there was no contamination by Ca^{2+}/Mg^{2+}.

We tested whether the difference between the old and new experiments might originate from an (unlikely) erroneous use of Na_2-EDTA instead of H-EDTA. The red curves in Fig. 1 B exclude that the negative slope is caused by the addition of Na^+. The Na^+ block shows a much sharper bending of the IV curve. Furthermore, in contrast to Ca^{2+}/Mg^{2+}, there is no reduction of current by Na^+ in the linear part of the IV curve. The IV curve with 10 mM H-EDTA obtained in Ca^{2+}/Mg^{2+}-free solution (Fig. 1 B, green curve) also excludes that EDTA could be the origin of the negative slope; it scarcely deviates from the black curve without EDTA.

There are some rare experimental indications that a contamination may not necessarily be the origin of the unusual IV curves in Schroeder and Hansen (2007). The most striking observation is shown in Fig. 1 C. During the recording of two subsequent IV curves in Kiel in Ca^{2+}/Mg^{2+}-free medium, the channel spontaneously switched from the "Ki-type" to the "Da-type" (increase of current) and remained there for the rest of the experiment. In addition, ∼10% of the experiments in Kiel showed "Da-type" behavior and vice versa. There was one notable difference between the records in the two

different laboratories. In Kiel, we rarely had more than one channel per patch; often there was not a single channel for a week. In Darmstadt, four channels in a patch were most common, and single channels were rare. This may indicate that the search for the differences of the IV curves in Fig. 1 B should not only be restricted to putative contaminations of the solutions but should also include the culturing conditions.

The evaluation of the flickering component by noise analysis

In the investigations of Schroeder and Hansen (2007), the effect of Ca^{2+}/Mg^{2+} on the IV curves of Fig. 1 B was not the main issue. Instead, the evaluation was based on the flickering component of BK currents, which becomes obvious in the excess open-channel noise shown in Fig. 1 A. This leads to the crucial question of whether the occurrence of different IV curves in the Ki-type data and in the Da-type data (Fig. 1 B) has any influence on the flickering.

Fig. 1 A shows nearly equal open-channel (excess) noise for the open-level with and without Ca^{2+}/Mg^{2+} in the new experiments. For the evaluation of the noise, open-point amplitude histograms were generated. In the examples of Fig. 2 A, the amplitude histogram without Ca^{2+}/Mg^{2+} is slightly broader than that obtained with Ca^{2+}/Mg^{2+}. However, such a visual inspection does not tell anything. The open-channel noise results from a convolution of the Gaussian baseline noise (C-level in Fig. 1 A, and dotted black line in Fig. 2 A) and the asymmetrical β distribution. The shape of the β distribution is influenced by the (strongly scattering) rate constants, and its broadness is weighted by the single-channel current. All these factors determine the shape of the histogram in such a complex manner that the only scientifically sound approach is a comparison of the parameters of flickering. They are provided by a β fit of the amplitude histograms as described in Materials and methods.

The analysis of the amplitude histogram by β distributions yields the "true" single-channel current (I_{true}) and the rate constants of the underlying flickering process (Schroeder and Hansen, 2006, 2009a,b; Brauser et al., 2012). The current I_{true} (for definition see Hansen et al., 2003) would be measured if a noise-free patch-clamp amplifier with a sufficient bandwidth were available. However, in our setup, the bandwidth is 20 kHz. Thus, if a flickering process in the microsecond range is present in the data, this low-pass filter averages over open and closed times, and a reduced value appears at the output of the amplifier: the apparent current I_{app}. I_{app} can be obtained from a visual inspection of the time series or from the peak of the open-point histograms (see Fig. 2 B). The occurrence of such a current reduction by undetected fast flickering is indicated by an increase of the noise (Fig. 1 A) of the open level ("excess noise"), which is higher than that of the closed level (baseline noise).

For the numerical analysis, the flickering process has to be defined by a Markov model. To test whether the flickering here is different from that in Schroeder and

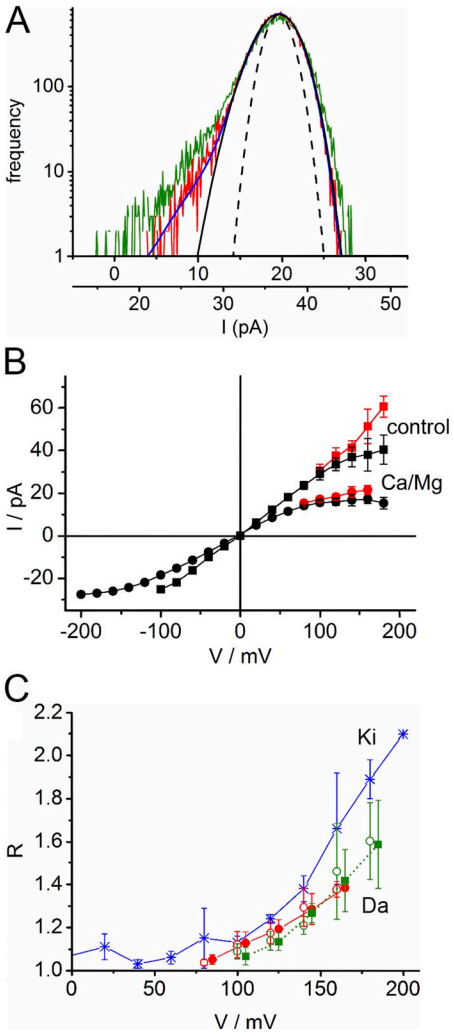

Figure 2. Analysis of fast flickering. (A) Superposition of two open-point amplitude histograms from time series at +140 mV with (red, mostly hidden behind the fit; black line, upper abscissa) and without (green, lower abcissa) Ca^{2+}/Mg^{2+}. Fitting the red one with a two-state model (black; Eq. 1) results in the following parameters: $I_{true} = 24$ pA, $k_{OC} = 0.44$ (µs)$^{-1}$, and $k_{CO} = 1.7$ (µs)$^{-1}$. Fitting with a three-state model (blue merging into black) C–O–G, with C,G being closed results in $I_{true} = 24$ pA, $k_{OC} = 0.49$ (µs)$^{-1}$, $k_{CO} = 2.00$ (µs)$^{-1}$, $k_{OG} = 0.005$ (µs)$^{-1}$, and $k_{GO} = 0.22$ (µs)$^{-1}$. The Gaussian distribution of the baseline (σ = 1.5 pA; black dashed, closed channel) is moved to $I_{app} = 19.6$ pA to illustrate the broadening by fast flickering. (B) Apparent (I_{app}, black) and true (I_{true}, red) single-channel IV curves for the recent experiments with (circles) and without (squares) divalent cations. (C) Results from the β fits of the open-point histograms at different membrane potentials (R_f, R_k; Eq. 2). Data from six different patches for each curve, with three to five data points per voltage. Data with Ca^{2+}/Mg^{2+} are shown in red, and data without divalent ions are shown in green. R_k is presented by closed symbols and shifted by 5 mV to avoid overlapping. The values of R_f are given by open symbols. Blue crosses, Ca^{2+}-independent R_k from Schroeder and Hansen (2007; "Ki").

Hansen (2007), we have to use the same model for the β analysis of the new data, namely, a two-state Markov C–O model, with the rate constants of the transitions being k_{CO} and k_{OC} (Eq. 1), and with I_{true} being the current level of the open state O and I_{min} = 0 pA the level of the closed state C.

The β fit is illustrated for the red amplitude histogram in the presence of Ca^{2+}/Mg^{2+} in Fig. 2 A. The narrow Gaussian curve in Fig. 2 A (black dashed) represents the baseline noise with a typical value of σ = 1.5 pA (shifted to I_{app}) for this dataset. The black continuous curve shows the β fit of the red amplitude histogram on the basis of Eq. 1. (The legitimate deviations at the left-hand side result from a second slower flickering process and can be evaluated by a three-state model [Schroeder and Hansen, 2009b]; see legend of Fig. 2 A.) The fit yields the "true" current I_{true} = 24.1 pA (as opposed to I_{app} = 19.6 pA), and the rate constants k_{OC} = 0.44 $(\mu s)^{-1}$ and k_{CO} = 1.7 $(\mu s)^{-1}$ of the open–close transitions in the two-state Markov model of Eq. 1 (averaged values are given below).

The comparison of the flickering component measured here and that reported by Schroeder and Hansen (2007) has to be based on the rate constants of the flickering process. However, as already known from the previous investigation, the determination of the rate constants themselves is subject to large scatter. In contrast, the ratio of the rate constants (R) is very reproducible. This flicker factor R can be calculated from the ratio of the currents (R_I) or from the rate constants (R_k), with

$$R_I = \frac{I_{true}}{I_{app}} \tag{2A}$$

and

$$R_k = \frac{k_{CO} + k_{OC}}{k_{CO}}. \tag{2B}$$

R_I and R_k should be identical if flickering is faster than can be resolved by the temporal resolution of the setup (Fig. 3 in Schroeder and Hansen, 2008). Then, the low-pass filter averages over the sojourns in the open and closed state of the flickering time series. The averaged open and closed times are the inverses of k_{OC} and k_{CO}, respectively. This leads to

$$\frac{1}{R_I} I_{true} = I_{app} = \frac{k_{CO}}{k_{OC} + k_{CO}} I_{true} = \frac{1}{R_k} I_{true}. \tag{3}$$

Fig. 2 C shows that R_k and R_I (open and closed symbols, respectively) fulfill the expectation of Eq. 3.

A surprising result: The reproducibility of the flickering component

The comparative analysis of fast flickering measured with and without Ca^{2+} and Mg^{2+} has led to a surprising result: Fig. 2 C shows that there is not a major difference in the flicker factors (R_I and R_k) between the recent experiments recorded with or without Ca^{2+}/Mg^{2+}. This implies that the behavior of the flicker factor shown in Fig. 2 C does not significantly differ between experiments that generate an almost linear IV curve (without divalent cations) and those with a strongly nonlinear IV curve (with divalent cations). Inspecting the red and black curves in Fig. 2 B seems to contradict the statement that $R_I = R_k$ is about equal with and without Ca^{2+}/Mg^{2+}. However, the greater difference between I_{true} and I_{app} without Ca^{2+}/Mg^{2+} results from the scaling by I_{true} (Eq. 2A).

With respect to the validity of the analysis in Schroeder and Hansen (2007), it is important to note that the values of R_k obtained here and in the previous investigation do not differ very much (Fig. 2 C, blue curve), even though the related IV curves of I_{app} shown in Fig. 1 B are quite different with respect to their sensitivity to Ca^{2+}/Mg^{2+}. This shows that current reduction by flickering and that by Ca^{2+}/Mg^{2+} block are unrelated processes.

An extended view of the single-channel currents at high temporal resolution

As mentioned above, the β analysis tells what would be measured if a noise-free patch-clamp amplifier of sufficient bandwidth were available. A bandwidth of 10 MHz would be sufficient because the fastest rate constant is k_{CO}. It scatters between 1 and 3 $(\mu s)^{-1}$ with a voltage-independent average value of k_{CO} = 1.33 $(\mu s)^{-1}$ without and 1.38 $(\mu s)^{-1}$ with 2.5 mM Ca^{2+}/Mg^{2+} calculated from 23 and 22 data points, respectively. The imaginary amplifier would show open events with average dwell times ranging from high values at 0 mV (hidden behind the normal gating dwell times in the millisecond range) to ∼1.4 µs at +180 mV (calculated from $1/k_{OC} = k_{CO}/(R_k - 1)$; Eq. 2B). These sojourns in the open state are interrupted by sojourns in the closed state with an average dwell time of $1/k_{CO}$ = 0.7 µs.

The imaginary 10-MHz amplifier also would show I_{true}, the "true" single-channel current not attenuated by the 20-kHz filter of the real amplifier. Fig. 2 B demonstrates that the IV curve of I_{true} does not show a negative slope in the presence of 2.5 mM Ca^{2+}/Mg^{2+} up to +160 mV. The current reduction by averaging in the filter of the real amplifier is given by R_I (Fig. 2 C and Eq. 2A). It is rather small; therefore, it causes only a minor sublinearity when the underlying "true" IV curve is linear (Fig. 2 B, without Ca^{2+}/Mg^{2+}). However, when the same percentage of current reduction occurs on the background of an already saturating true IV curve, a negative slope can result. Thus, Schroeder and Hansen (2007; for BK channels) and Abenavoli et al. (2009; for the viral Kcv channel) found a saturating IV curve of I_{true}, where I_{app} showed already a very pronounced negative slope. In Fig. 2 B, the saturating IV curve for I_{true} in the presence of 2.5 mM Ca^{2+}/Mg^{2+} is only proven up to +160 mV, but extrapolation of R_I in Fig. 2 C suggests a similar picture.

Conclusion

IV curves in BK channels measured with and without Ca^{2+}/Mg^{2+} reported here are the same as those reported by Geng et al. (2013) in contrast to previous findings of Schroeder and Hansen (2007). However, the discrepancy regarding the IV curves has no effect on the phenomenon that is in the focus of Schroeder and Hansen (2007): the flickering process in the microsecond range. It is the same here and in those previous studies. Thus, the experimental basis for the analysis in Schroeder and Hansen (2007) is sound. With respect to the IV curves, the analysis of flickering has to be included because it yields a refined picture of the block by 2.5 mM Ca^{2+}/Mg^{2+}. The block per se causes saturating IV curves at least up to +160 mV. Bending downward is further enhanced by the decrease of apparent current as caused by averaging over voltage-dependent flickering at high positive potentials.

Thanks are due to Karl Magleby (University of Miami), who insisted on a reanalysis of the findings from Schroeder and Hansen (2007), thus leading us to the detection of the two independent components. He contributed many helpful suggestions to the manuscript.

These investigations were supported by the Deutsche Forschungsgemeinschaft (Ha 712/14-3) and by Loewe Cluster Soft-Control (Technical University of Darmstadt, Germany).

Lawrence G. Palmer served as editor.

Submitted: 28 December 2012
Accepted: 1 March 2013

REFERENCES

Abenavoli, A., M.L. DiFrancesco, I. Schroeder, S. Epimashko, S. Gazzarrini, U.P. Hansen, G. Thiel, and A. Moroni. 2009. Fast and slow gating are inherent properties of the pore module of the K^+ channel Kcv. *J. Gen. Physiol.* 134:219–229. http://dx.doi.org/10.1085/jgp.200910266

Brauser, A., I. Schroeder, T. Gutsmann, C. Cosentino, A. Moroni, U.P. Hansen, and M. Winterhalter. 2012. Modulation of enrofloxacin binding in OmpF by Mg^{2+} as revealed by the analysis of fast flickering single-porin current. *J. Gen. Physiol.* 140:69–82. http://dx.doi.org/10.1085/jgp.201210776

Brelidze, T.I., and K.L. Magleby. 2004. Protons block BK channels by competitive inhibition with K^+ and contribute to the limits of unitary currents at high voltages. *J. Gen. Physiol.* 123:305–319. http://dx.doi.org/10.1085/jgp.200308951

Cox, D.H., J. Cui, and R.W. Aldrich. 1997. Separation of gating properties from permeation and block in *mslo* large conductance Ca-activated K^+ channels. *J. Gen. Physiol.* 109:633–646. http://dx.doi.org/10.1085/jgp.109.5.633

Draber, S., and U.P. Hansen. 1994. Fast single-channel measurements resolve the blocking effect of Cs^+ on the K^+ channel. *Biophys. J.* 67:120–129. http://dx.doi.org/10.1016/S0006-3495(94)80461-8

Ferguson, W.B. 1991. Competitive Mg^{2+} block of a large-conductance, Ca^{2+}-activated K^+ channel in rat skeletal muscle. Ca^{2+}, Sr^{2+}, and Ni^{2+} also block. *J. Gen. Physiol.* 98:163–181. http://dx.doi.org/10.1085/jgp.98.1.163

FitzHugh, R. 1983. Statistical properties of the asymmetric random telegraph signal, with applications to single-channel analysis. *Math. Biosci.* 64:75–89. http://dx.doi.org/10.1016/0025-5564(83)90028-7

Geng, Y., X. Wang, and K.L. Magleby. 2013. Lack of negative slope in I-V plots for BK channels at positive potentials in the absence of intracellular blockers. *J. Gen. Physiol.* 141:493–497.

Hansen, U.P., O. Cakan, M. Abshagen-Keunecke, and A. Farokhi. 2003. Gating models of the anomalous mole-fraction effect of single-channel current in *Chara*. *J. Membr. Biol.* 192:45–63. http://dx.doi.org/10.1007/s00232-002-1063-z

Heinemann, S.H., and F.J. Sigworth. 1991. Open channel noise. VI. Analysis of amplitude histograms to determine rapid kinetic parameters. *Biophys. J.* 60:577–587. http://dx.doi.org/10.1016/S0006-3495(91)82087-2

Kehl, S.J. 1996. Block of BK (maxi K) channels of rat pituitary melanotrophs by Na^+ and other alkali metal ions. *Pflugers Arch.* 432:623–629. http://dx.doi.org/10.1007/s004240050178

Lu, R., A. Alioua, Y. Kumar, M. Eghbali, E. Stefani, and L. Toro. 2006. MaxiK channel partners: physiological impact. *J. Physiol.* 570:65–72. http://dx.doi.org/10.1113/jphysiol.2005.098913

Magleby, K.L. 2003. Gating mechanism of BK (Slo1) channels: So near, yet so far. *J. Gen. Physiol.* 121:81–96. http://dx.doi.org/10.1085/jgp.20028721

Morales, E., W.C. Cole, C.V. Remillard, and N. Leblanc. 1996. Block of large conductance Ca^{2+}-activated K^+ channels in rabbit vascular myocytes by internal Mg^{2+} and Na^+. *J. Physiol.* 495:701–716.

Orio, P., and R. Latorre. 2005. Differential effects of β1 and β2 subunits on BK channel activity. *J. Gen. Physiol.* 125:395–411. http://dx.doi.org/10.1085/jgp.200409236

Pallotta, B.S., K.L. Magleby, and J.N. Barrett. 1981. Single channel recordings of Ca^{2+}-activated K^+ currents in rat muscle cell culture. *Nature.* 293:471–474. http://dx.doi.org/10.1038/293471a0

Piskorowski, R.A., and R.W. Aldrich. 2006. Relationship between pore occupancy and gating in BK potassium channels. *J. Gen. Physiol.* 127:557–576. http://dx.doi.org/10.1085/jgp.200509482

Riessner, T. 1998. Level Detection and Extended Beta Distributions for the Analysis of Fast Rate Constants of Markov Processes in Sampled Data. Shaker-Verlag, Aachen, Germany. 74 pp.

Rothberg, B.S., and K.L. Magleby. 2000. Voltage and Ca^{2+} activation of single large-conductance Ca^{2+}-activated K^+ channels described by a two-tiered allosteric gating mechanism. *J. Gen. Physiol.* 116:75–99. http://dx.doi.org/10.1085/jgp.116.1.75

Schröder, I., T. Huth, V. Suitchmezian, J. Jarosik, S. Schnell, and U.P. Hansen. 2004. Distributions-per-level: a means of testing level detectors and models of patch-clamp data. *J. Membr. Biol.* 197:49–58. http://dx.doi.org/10.1007/s00232-003-0641-z

Schroeder, I., and U.P. Hansen. 2006. Strengths and limits of Beta distributions as a means of reconstructing the true single-channel current in patch clamp time series with fast gating. *J. Membr. Biol.* 210:199–212. http://dx.doi.org/10.1007/s00232-006-0858-8

Schroeder, I., and U.P. Hansen. 2007. Saturation and microsecond gating of current indicate depletion-induced instability of the MaxiK selectivity filter. *J. Gen. Physiol.* 130:83–97. http://dx.doi.org/10.1085/jgp.200709802

Schroeder, I., and U.P. Hansen. 2008. Tl^+-induced μs gating of current indicates instability of the MaxiK selectivity filter as caused by ion/pore interaction. *J. Gen. Physiol.* 131:365–378. http://dx.doi.org/10.1085/jgp.200809956

Schroeder, I., and U.P. Hansen. 2009a. Interference of shot noise of open-channel current with analysis of fast gating: patchers do not (Yet) have to care. *J. Membr. Biol.* 229:153–163. http://dx.doi.org/10.1007/s00232-009-9183-3

Schroeder, I., and U.P. Hansen. 2009b. Using a five-state model for fitting amplitude histograms from MaxiK channels: β-distributions reveal more than expected. *Eur. Biophys. J.* 38:1101–1114. http://dx.doi.org/10.1007/s00249-009-0515-0

Schultze, R., and S. Draber. 1993. A nonlinear filter algorithm for the detection of jumps in patch-clamp data. *J. Membr. Biol.* 132:41–52.

Weise, R., and D. Gradmann. 2000. Effects of Na^+ on the predominant K^+ channel in the tonoplast of *Chara*: decrease of conductance

by blocks in 100 nanosecond range and induction of oligo- or poly-subconductance gating modes. *J. Membr. Biol.* 175:87–93. http://dx.doi.org/10.1007/s002320001057

Xia, X.M., X. Zeng, and C.J. Lingle. 2002. Multiple regulatory sites in large-conductance calcium-activated potassium channels. *Nature.* 418:880–884. http://dx.doi.org/10.1038/nature00956

Xia, X.M., X. Zhang, and C.J. Lingle. 2004. Ligand-dependent activation of Slo family channels is defined by interchangeable cytosolic domains. *J. Neurosci.* 24:5585–5591. http://dx.doi.org/10.1523/JNEUROSCI.1296-04.2004

Yang, H., L. Hu, J. Shi, and J. Cui. 2006. Tuning magnesium sensitivity of BK channels by mutations. *Biophys. J.* 91:2892–2900. http://dx.doi.org/10.1529/biophysj.106.090159

Yellen, G. 1984. Ionic permeation and blockade in Ca^{2+}-activated K^+ channels of bovine chromaffin cells. *J. Gen. Physiol.* 84:157–186. http://dx.doi.org/10.1085/jgp.84.2.157

Zhang, Y., X. Niu, T.I. Brelidze, and K.L. Magleby. 2006. Ring of negative charge in BK channels facilitates block by intracellular Mg^{2+} and polyamines through electrostatics. *J. Gen. Physiol.* 128:185–202. http://dx.doi.org/10.1085/jgp.200609493